



Three Phase Grid-Connected Photovoltaic System using Three Level H-bridge Inverter under Partial Shading

G.G SIRISHA RATNA BHARGAVI

Department of Electrical & Electronics Engineering
JNT University Kakinada
Kakinada, India.

H.SIREESHA

Department of Electrical & Electronics Engineering
JNT University Kakinada
Kakinada, India.

Abstract— This paper deals with three-phase three level H bridge inverter for a photovoltaic power plant interconnected to grid under variable irradiation conditions, that features a maximum power point tracking scheme based on the Perturb and Observe (P&O) method. With the aid of the sinusoidal pulse-width modulation control technique, proportional-integral controllers, and Park transformation, the inverter control system managed to convert photovoltaic power to ac power, stabilize the output voltage and current of a grid connected photovoltaic system. The photovoltaic module has been modelled, the maximum power point tracking algorithm and a three level inverter has been validated by simulation analysis. The simulation results show the detailed model of this grid-connected multi-level inverter and the control strategy used in the photovoltaic generation system.

Keywords- PV Array, Perturb and Observe MPPT, PWM H-bridge Inverter, Synchronous reference frame theory.

I. INTRODUCTION

Due to shortage of fossil fuels and environmental problems caused by conventional power generation, renewable energy, especially solar energy, has become very popular. Solar-electric-energy demand has grown consistently by 20%-25% per annum over the past 20 years [1], and the growth is mostly in grid-connected applications. With the extraordinary market growth in grid-connected PV systems, there is increasing interests in grid-connected PV configurations.

The PV system consists of the control system, inverter which interfaces the PV and the grid, harmonic filter, and PV power simulator featuring the maximum power point tracking (MPPT) function.

A modular H-bridge multilevel inverter topology for three-phase grid-connected PV systems is presented in this paper. The panel mismatch issues are addressed to show the necessity of individual MPPT control, and a control scheme with distributed MPPT control is then proposed. The distributed MPPT control scheme can be applied to three-phase systems.

In addition, for the presented three-phase grid-connected PV system, PV mismatches may introduce unbalanced power supplied to the three-phase multilevel inverter, leading to unbalanced injected grid current. To balance the three-phase grid current, modulation compensation is also added to the control system.

A three-phase modular multilevel inverter prototype has been simulated. Each H-bridge is connected to a 1000 W solar panel. The modular

design will increase the flexibility of the system, and reduce the cost as well.

The proposed photovoltaic array simulation model to be used in Matlab/Simulink environment is developed. The model is using basic circuit equation of the photovoltaic solar cells at constant temperature and variable solar irradiation. In this paper the perturb and observe MPPT technique is discussed and Based on the regular sampled three-phase SPWM strategy, H-bridge multilevel inverter [2] has been constructed.

II. SOLAR CELL MODELING

Solar cells consist of a p-n junction fabricated in thin wafer or layer of semiconductors, whose electrical characteristics differ very little from a diode represented by the equation of Shockley [3]. Thus the simplest equivalent circuit of a solar cell is a current source in parallel with a diode as shown in Fig . 1. The output of the current source is directly proportional to the light falling on the cell (photocurrent $I_{pv, cell}$) .So the process of modeling this solar cell can be developed based on (1) :

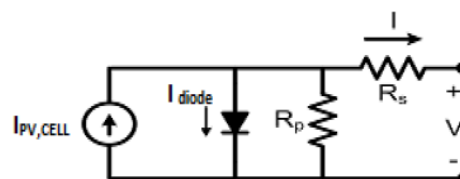


Figure 1. Equivalent Model of a Photovoltaic Cell.

$$I = I_{PV, CELL} - I_{diode}$$

$$= I_{PV,CELL} - I_{0,CELL} \left[\exp \left(\frac{q * V}{\alpha * k * T} \right) - 1 \right] \quad (1)$$

$I_{PV,CELL}$ is the current generated by the incident light. I_{diode} is the Shockley diode equation.

$I_{0,CELL}$ is the leakage current of the diode [A].

q is the electron charge [$1.60217646 * 10^{-19}$ C].

k is the Boltzmann constant [$1.3806503 * 10^{-23}$ J/K].

T is the temperature of the p-n junction.

α is the diode ideality constant which lies between 1 and 2 for mono crystalline silicon.

The basic equation (1) of the elementary PV does not represent the I-V characteristic of practical PV arrays. Practical modules are composed of several connected PV cells requires the inclusion of additional parameters series resistance (R_s) and parallel resistance (R_p), with these parameters (1) becomes (2)

$$I = I_{PV} - I_0 \left[\exp \left(\frac{V + R_s * I}{V_t * \alpha} \right) - 1 \right] - \frac{V + R_s * I}{R_p} \quad (2)$$

where

$$I_{PV} = (I_{PV} + K_1 \Delta T) \frac{G}{G_n} \quad (3)$$

Where K_1 is the Temperature coefficient of I_{sc} , G is the irradiance (W/m^2) and G_n is the irradiance at standard operating conditions.

$$I_0 = I_{0,n} \left(\frac{T_n}{T} \right)^3 \exp \left[\frac{q * E_g}{\alpha * k} \left(\frac{1}{T_n} - \frac{1}{T} \right) \right] \quad (4)$$

E_g is the band gap energy of the semiconductor and $I_{0,n}$ is the nominal saturation current expressed by (5).

$$I_{0,n} = \frac{I_{sc,n}}{\exp \left(\frac{V_{oc,n}}{V_{t,n} * \alpha} \right) - 1} \quad (5)$$

Where $V_{oc,n}$ is open circuit voltage, $I_{sc,n}$ is the short circuit current, $V_{t,n}$ is the thermal voltage, T_n is the temperature at standard operating conditions.

$$V_t = N_s * \frac{K_T}{q}$$

is the thermal voltage of the module with N_s cells connected in series.

The characteristic curves of the PV array system depend on the radiation and temperature of the PV system[4],[5],[6]. For a given system, during normal conditions where the radiation is equally distributed among the PV modules, the power-duty cycle ($P-D$) characteristics under varying weather conditions are shown in Fig. 2(a) and 2(b).

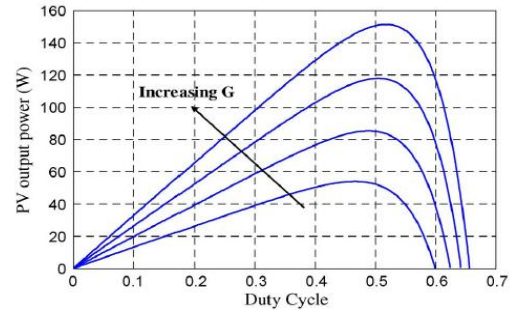


Figure 2(a). Influences of solar radiation (G) on the $P-D$ characteristics.

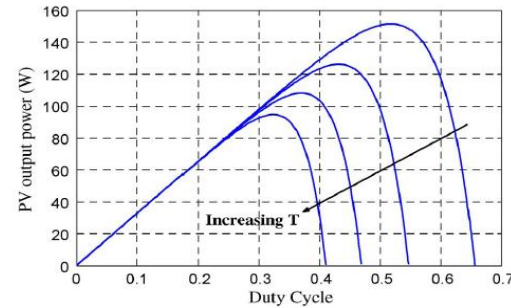


Figure 2(b). Influences of temperature (T) on the $P-D$ characteristics.

However, when the radiation is not equally distributed, local and global maxima are introduced in the characteristic curves. In order to understand such phenomena, a PV array system with nine modules connected in series and parallel is considered, as shown in Fig. 3.

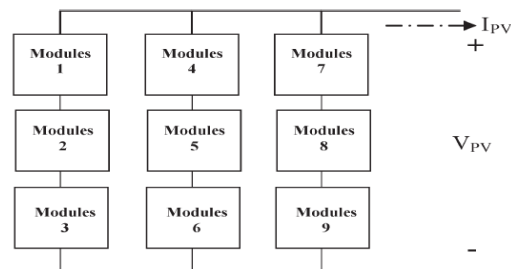


Figure 3. PV array system with nine modules connected in series and parallel.

There are different possibilities for the radiation distribution among the PV modules; the following five cases are randomly considered.

- Case1) Three modules in a column is 50% shaded (viz., modules 1, 2, and 3) i.e. of irradiation $500W/m^2$.
- Case2) Three modules in a column is completely shaded (viz., modules 1, 2, and 3)
- Case3) Each string is partially shaded with unequal radiation levels.
- Case4) Three modules in the first and second column are completely shaded (viz., modules 1, 2, 3, 4, 5, and 6) and third

column of irradiation 1000W/m² (viz., modules 7,8, and 9).

Simulation results for the four cases indicate that a completely shaded module causes a reduction of the PV output power without creating local maxima. However, partially shaded modules result in a reduction of the PV output power, creating local maxima, where the number of local maxima increases as the variation of the radiation levels on each module increases.

III. PERTURB AND OBSERVE ALGORITHM

MPPT algorithms are necessary in PV applications because the MPP of a solar panel varies with the irradiation and temperature, so the use of MPPT algorithms is required in order to obtain the maximum power from a solar array. There are many MPPT techniques. The most commonly used MPPT algorithm is P&O method. This algorithm uses simple feedback arrangement and little measured parameters. In this approach, the module voltage is periodically given a perturbation and the corresponding output power is compared with that at the previous perturbing cycle [7]. In this algorithm a slight perturbation is introduced to the system. This perturbation causes the power of the solar module varies. If the power increases due to the perturbation then the perturbation is continued in the same direction. After the peak power is reached the power at the MPP is zero and next instant decreases and hence after that the perturbation reverses as shown in Fig. 4(a) and 4(b).

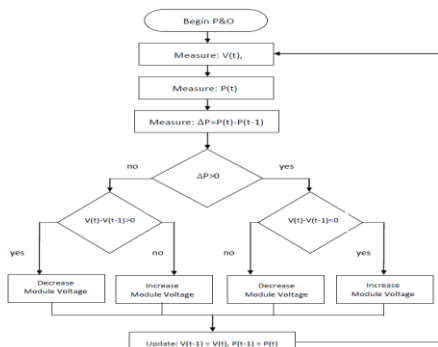


Figure 4(a). P&O Algorithm

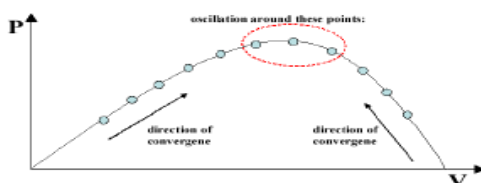


Figure 4(b). Graph Power versus Voltage

IV. THREE LEVEL H-BRIDGE INVERTER

The H bridge inverter is a multi-level inverter that has been widely used in high voltage fields. By increasing the number of levels in a given topology,

the output voltages in the case of VSI, and output currents in the case of CSI, assume stair-case waveforms with increased number of steps.

A. Topology

The three phase three level inverter topology consists of three H-bridge inverters [8] and is shown in Fig. 5. Each DC link is fed by a short string of PV panels. By different combinations of the four switches in each H bridge, three output voltage levels can be generated, $-v_c$, 0, or $+v_c$.

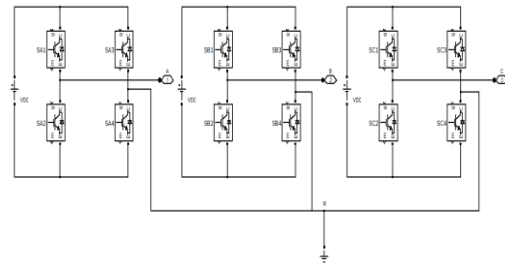


Figure 5. Three level H-bridge inverter

PWM techniques are represented by fixed amplitude pulses. This is the most suitable method of controlling the output PWM techniques are represented by fixed amplitude pulses. This is the most suitable method of controlling the output voltage. This method is labelled as Pulse-Width Modulation (PWM) Control. The advantages entailed by PWM techniques are mentioned in: [9], [10]. The various PWM techniques are as following: a) Single-pulse modulation b) Multiple pulse modulation c) Sinusoidal pulse width modulation. Fig. 6. shows the phase disposition PWM technique for a three level inverter.

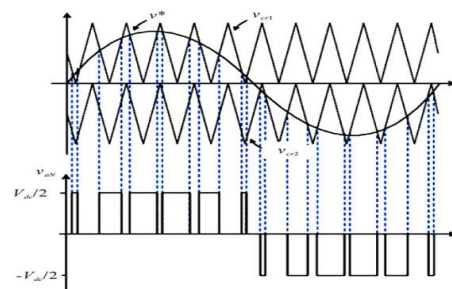


Figure 6. Phase disposition PWM technique

V. GRID SYNCHRONIZATION AND ITS CONTROL STRATEGY

Grid inverter needs a pure sinusoidal reference voltage to ensure that the sinusoidal output of the inverter is synchronized to the grid frequency.

The control strategy applied for inverter consists of two control loops. Usually there is a fast inner control loop which controls grid current and an external voltage loop which control dc link voltage. The current control loop is responsible for power quality issues like low THD and good power factor, whereas voltage control loop balances the power

flow in the system. Synchronous reference frame control [11],[12],[13] also called d-q control uses a reference frame transformation abc to dq which transforms the grid current and voltages into d-q frame. After that, the stationary frame quantities are transferred into synchronous rotating frames using cosine and sinus functions from the phase-locked loop (PLL)[14],[15]. The sinus and cosine functions help to maintain the synchronization with supply voltage and current. The transformed voltage detects phase and frequency of grid, whereas transformed current controls the grid current. Thus the control variables becomes dc values, hence filtering and controlling becomes easier.

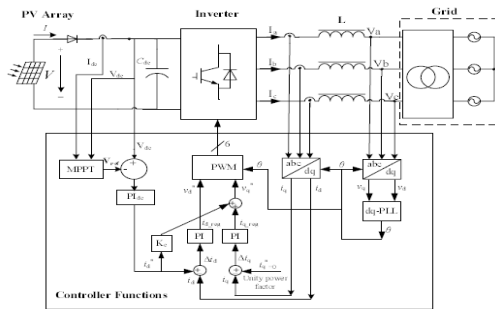


Figure 7. Configuration of grid connected PV system

The schematic of the d-q control is shown in Fig. 7. In equations (8) and (9), the grid voltages V_{abc} and the inverter currents I_{abc} are transformed $d-q-0$ by using the transformation matrix T given in (6).

$$T = \frac{2}{3} \begin{bmatrix} \frac{1}{\sqrt{2}} & \frac{1}{\sqrt{2}} & \frac{1}{\sqrt{2}} \\ \sin(\omega t) & \sin(\omega t - \frac{2\pi}{3}) & \sin(\omega t + \frac{2\pi}{3}) \\ \cos(\omega t) & \cos(\omega t - \frac{2\pi}{3}) & \cos(\omega t + \frac{2\pi}{3}) \end{bmatrix} \quad (6)$$

$$T^{-1} = \frac{2}{3} \begin{bmatrix} \frac{1}{\sqrt{2}} & \sin(\omega t) & \cos(\omega t) \\ \frac{1}{\sqrt{2}} & \sin(\omega t - \frac{2\pi}{3}) & \cos(\omega t - \frac{2\pi}{3}) \\ \frac{1}{\sqrt{2}} & \sin(\omega t + \frac{2\pi}{3}) & \cos(\omega t + \frac{2\pi}{3}) \end{bmatrix} \quad (7)$$

$$\begin{bmatrix} V_o \\ V_d \\ V_q \end{bmatrix} = T \begin{bmatrix} V_a \\ V_b \\ V_c \end{bmatrix} \quad (8)$$

$$\begin{bmatrix} I_o \\ I_d \\ I_q \end{bmatrix} = T \begin{bmatrix} I_a \\ I_b \\ I_c \end{bmatrix} \quad (9)$$

The inverter reference voltages (V_{abc}) are calculated as in (10). The inverse transformation matrix T^{-1} in (7) is used for producing the reference voltages by the average component of source voltage and ωt produced in the modified PLL algorithm.

$$\begin{bmatrix} V_a \\ V_b \\ V_c \end{bmatrix} = T^{-1} \begin{bmatrix} 0 \\ V_d \\ V_q \end{bmatrix} \quad (10)$$

The DC link voltage is actually fed from PV. The reference for active current control is set by DC link voltage, whereas reactive power control reference is set to zero, as reactive power control is not done here. If reactive power has to be controlled a reference must be set in the system for that also.

VI. SIMULATION ANALYSIS

Here the simulation is carried out of Three phase three level H bridge inverter for grid connected photovoltaic system at a temperature of 25°C and an irradiance of 1000W/m². Simulation circuit of three phase multi level inverter for grid connected PV system is shown in Fig. 8.

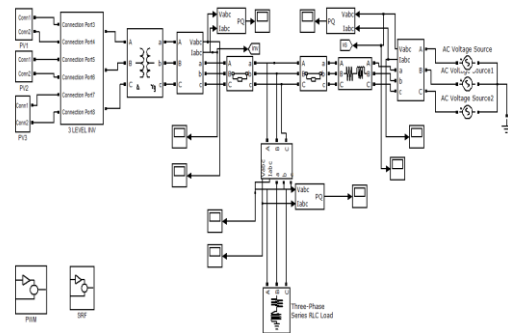


Figure 8. Three phase multi level inverter for grid connected PV system.

PV sub system has been considered and its electrical characteristics are in Table I and the MPPT algorithm includes Perturb and Observe method is applied to this system.

TABLE I: SPECIFICATIONS OF THE SOLAR ARRAY AT 25°C, 1000W/M²

Specifications	Values
Maximum Power (P_{max})	1372.14W
Voltage at Pmax (V_{mp})	108V
Current at Pmax (I_{mp})	12.705A
Open-circuit voltage(V_{oc})	130.2V
Short-circuit current (I_{sc})	13.2A
Temperature coefficient of I_{sc}	(0.0032±0.015)%/°C
Temperature coefficient of V_{oc}	-80±10mV/°C

The parameters for the grid and inverter are shown in Table II. The following parameters are used in the filter design.

TABLE II: PARAMETERS OF PV GRID-CONNECTED SYSTEM

Parameters	Values
Grid line voltage(V_{L-L})	415Vrms
Grid phase voltage(V_{ph})	240Vrms
DC source voltage(V_{dc})	100V
DC current (I_{dc})	10A
Output power fed to grid(P_n)	1000W
Grid frequency (f)	50Hz
Switching frequency(f_s)	1KHz
Filter inductor	70mH
Filter Capacitor	60 μ F
Parameters PI	$K_p=10, K_i=0.02$

The DC voltage, current and power are shown in Fig. 9(a),9(b),9(c). respectively.

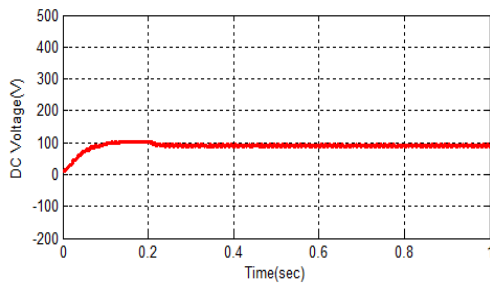


Figure 9(a). DC voltage of PV array

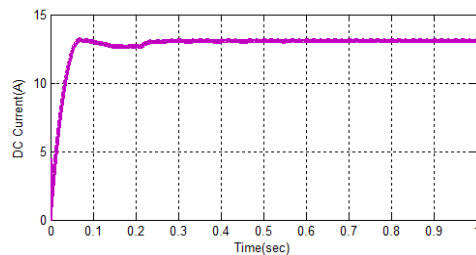


Figure 9(b). DC current of PV array

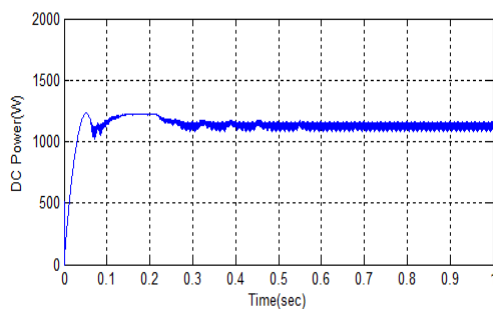


Figure 9(c). DC Power of PV array

Load of Power factor unity .Fig. 10(a), 10(b),10(c) shows output active and reactive power of inverter, grid and load respectively.

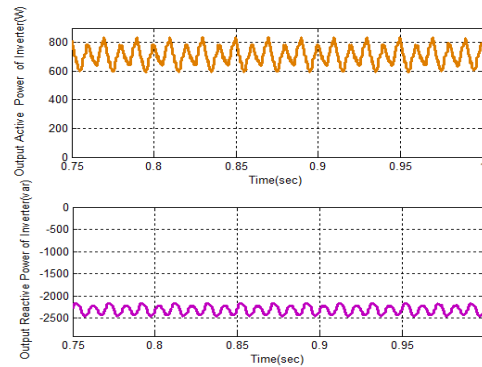


Figure 10(a). Output active and reactive power of Inverter

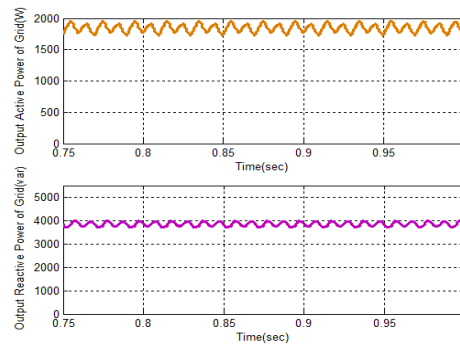


Figure 10(b). Output active and reactive power of Grid.

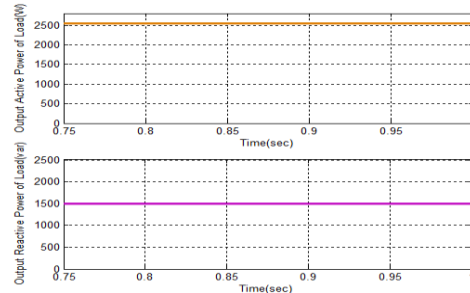


Figure 10(c). Output active and reactive power of Load.

Under Partial shaded conditions , the active and reactive power of inverter ,grid and load are shown below.

Case.1(a): A string in a photovoltaic Array is 50% shaded with an irradiance of 500W/m² and at constant temperature 25°C is connected to Load of Power factor unity .Fig. 11(a), 11(b), 11(c) shows output active and reactive power of inverter, grid and load respectively.

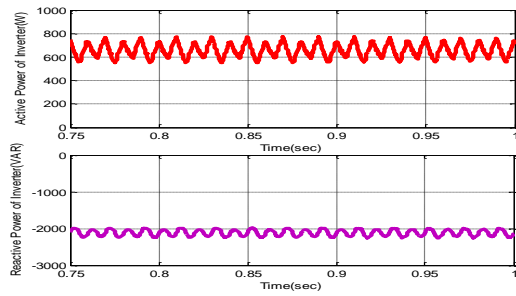


Figure 11(a). Output active and reactive power of Inverter

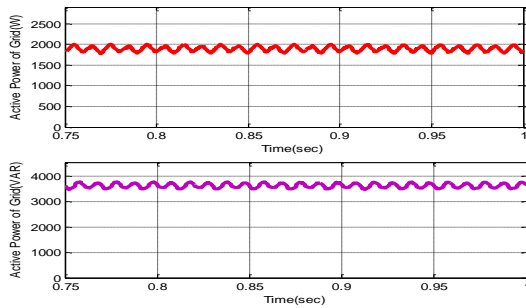


Figure 11(b). Output active and reactive power of Grid.

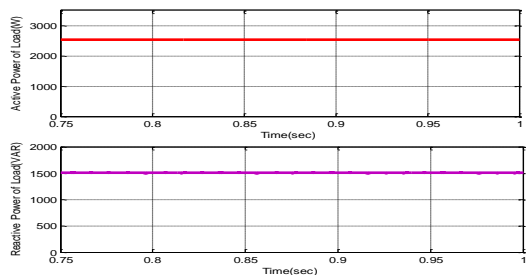


Figure 11(c). Output active and reactive power of Load.

Case.1(b): The same PV array is connected to Load of Power factor 0.75 .Fig. 12(a),12(b),12(c)shows output active and reactive power of inverter, grid and load respectively.

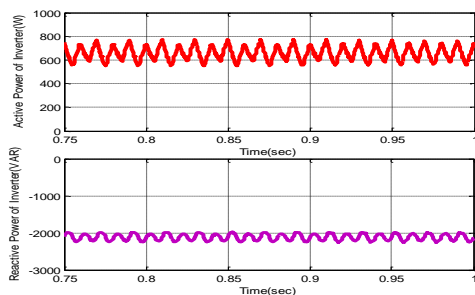


Figure 12(a). Output active and reactive power of Inverter.

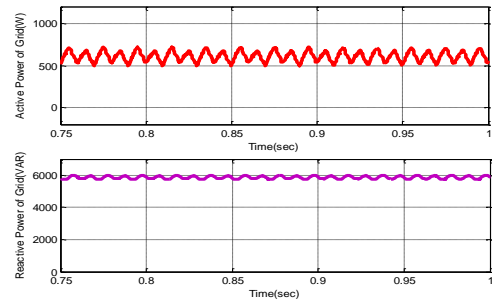


Figure 12(b). Output active and reactive power of Grid.

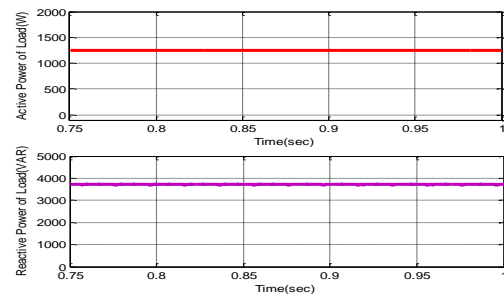


Figure 12(c). Output active and reactive power of Load.

Case.2(a): A string in a photovoltaic Array is completely shaded and at constant temperature 25°C is connected to Load of Power factor unity. Fig. 13(a), 13(b),13(c) shows output active and reactive power of inverter, grid and load respectively.

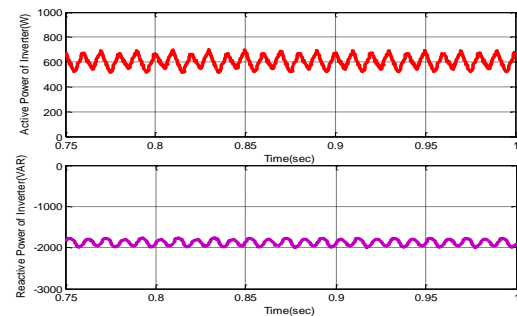


Figure 13(a). Output active and reactive power of Inverter

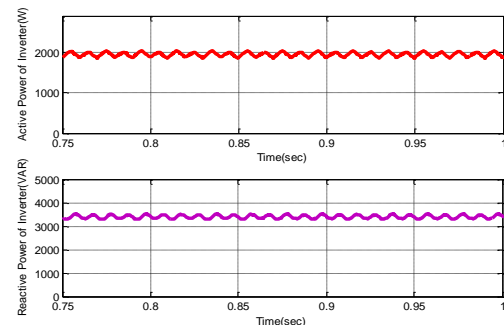


Figure 13(b). Output active and reactive power of Grid.

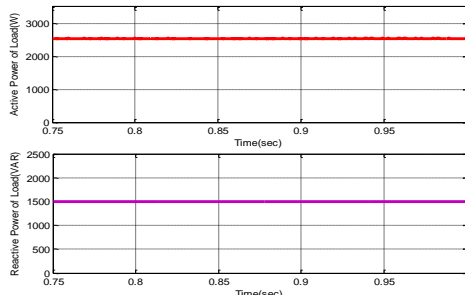


Figure 13(c). Output active and reactive power of Load.

Case 2(b): The same PV array is connected to Load of Power factor 0.75 .Fig. 14(a), 14(b),14(c) shows output active and reactive power of inverter, grid and load respectively.

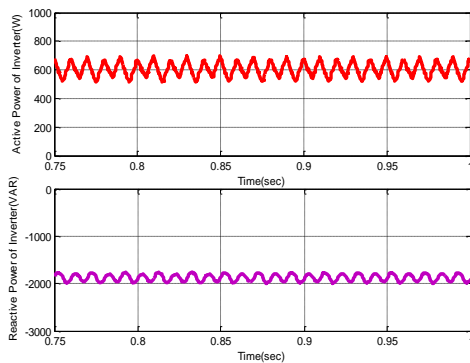


Figure 14(a). Output active and reactive power of Inverter

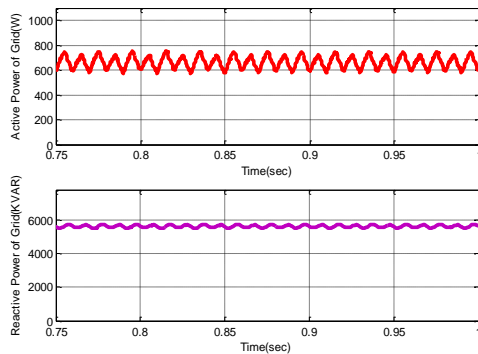


Figure 14(b). Output active and reactive power of Grid.

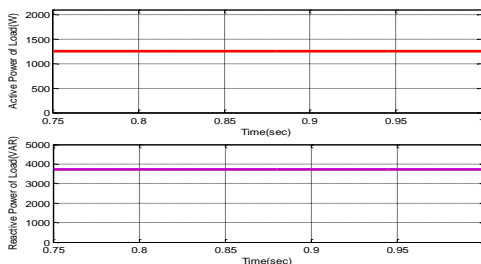


Figure 14(c). Output active and reactive power of Load.

Case.3(a): Let us consider a string in a photovoltaic Array with an irradiance of 500W/m^2 and a string is completely shaded and at constant temperature 25°C is connected to Load of Power

factor unity. Fig. 15(a),15(b),15(c)shows output active and reactive power of inverter, grid and load respectively.

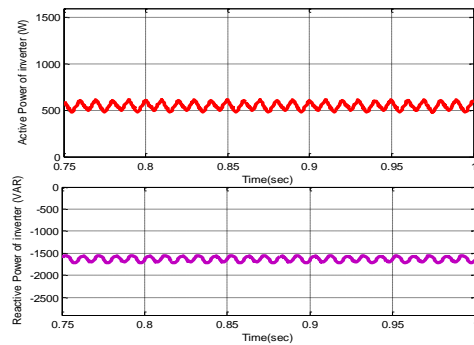


Figure 15(a). Output active and reactive power of Inverter

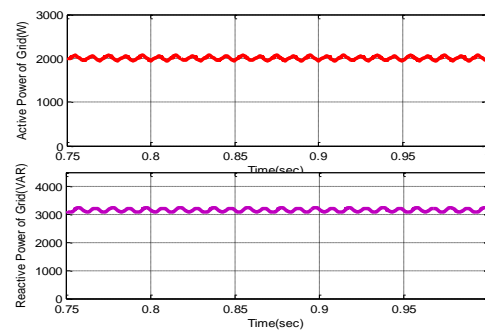


Figure 15(b). Output active and reactive power of Grid.

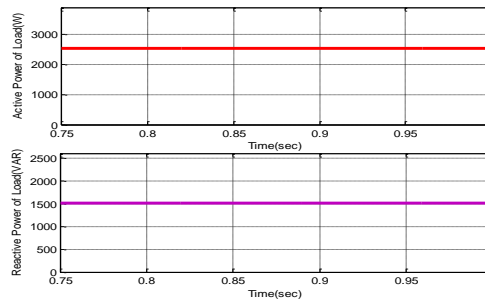


Figure 15(c). Output active and reactive power of Load.

Case.3(b): The same PV array is connected to Load of Power factor 0.75.Fig. 16(a),16(b),16(c) shows output active and reactive power of inverter, grid and load respectively.

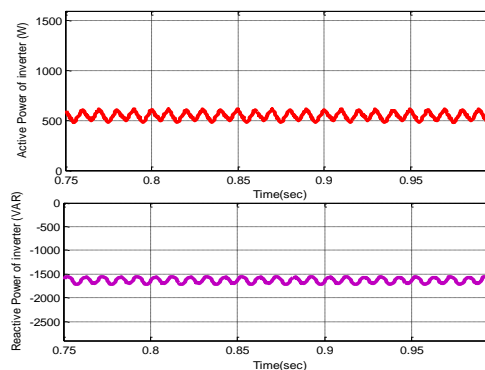


Figure 16(a). Output active and reactive power of Inverter.

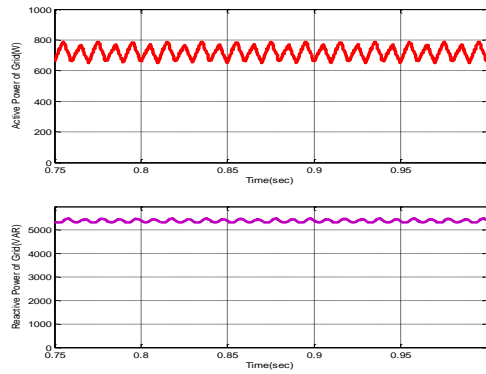


Figure 16(b). Output active and reactive power of Grid.

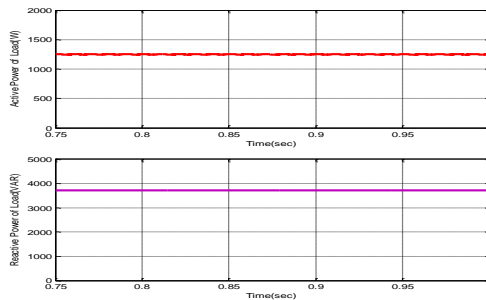


Figure 16(c). Output active and reactive power of Load.

Case 4(a): Let us consider a string in a photovoltaic Array with an irradiance of 1000W/m^2 and two strings are completely shaded and at constant temperature 25°C is connected to Load of Power factor unity. Fig. 17(a),17(b),17(c) shows output active and reactive power of inverter, grid and load respectively.

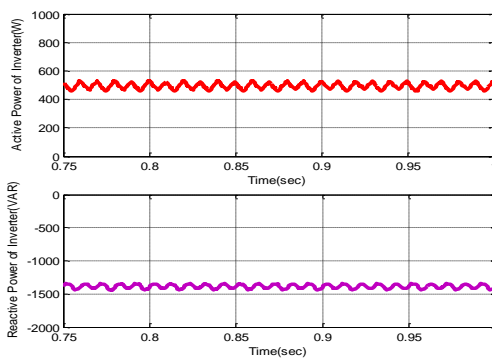


Figure 17(a). Output active and reactive power of Inverter.

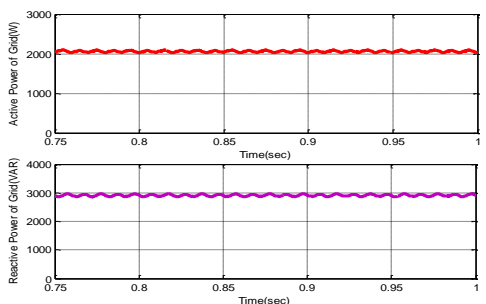


Figure 17(b). Output active and reactive power of Grid.

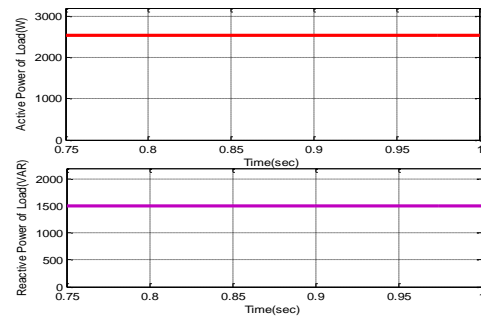


Figure 17(c). Output active and reactive power of Load.

Case 4(b): The same PV array is connected to Load of Power factor 0.75. Fig. 18(a),18(b),18(c) shows output active and reactive power of inverter, grid and load respectively.

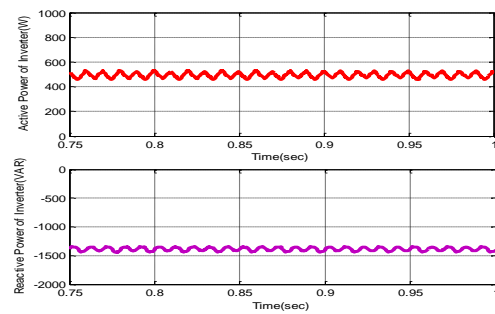


Figure 18(a). Output active and reactive power of Inverter.

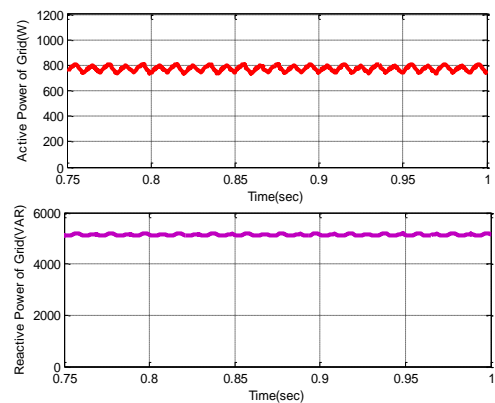


Figure 18(b). Output active and reactive power of Grid.

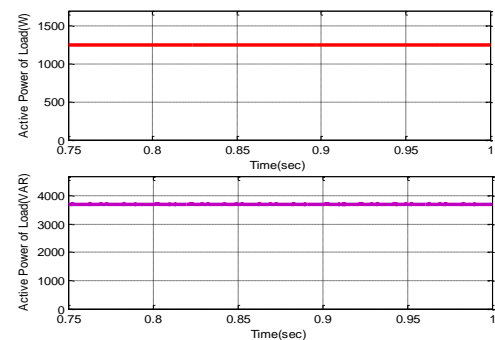


Figure 18(c). Output active and reactive power of Load.

VII. CONCLUSION

The three phase photovoltaic grid-connected generation system with MPPT function is proposed. According to the equivalent circuit of the PV array, it builds the mathematic model of photovoltaic array. Presented results showed that the inverter and its control design are successful in converting PV dc power to ac power for supplying power to the load. Also, the simulation results for different loading conditions are shown, where output power of inverter that is PV power remains constant. And the excess power required for load is being drawn from the grid.

VIII. REFERENCES

- [1] Hurng-Liahng Iou, Wen-Iung Chiang, et al, "Voltage-mode grid-connected solar inverter with high frequency isolated transformer," IEEE International Symposium on Industrial Electronics, 2009, pp. 1087-1092.
- [2] Xianglian Xu, Qing Zhang, Qian Cheng, Youxin Yuan, Yiping Xiao. "An Auto-disturbance Rejection Controller for STATCOM Based on Cascaded Multilevel Inverters," 2009 IEEE 6th International Power Electronics and Motion Control Conference, Wuhan, China, DS11.4, 2349-2353.
- [3] M.G. Villalva, J.R. Gazoli and E.R. Filho, —Comprehensive approach to modeling and simulation of photovoltaic arrayl, IEEE Trans on Power Electronics, Vol. 24, n°5, pp.1198-1208, May 2009 .
- [4] G. Lijun, R. A. Dougal, L. Shengyi, and A. P. Iotova, "Parallel-connected solar PV system to address partial and rapidly fluctuating shadow conditions," *IEEE Trans. Ind. Electron.*, vol. 56, no. 5, pp. 1548–1556, May 2009.
- [5] T. L. Nguyen and K.-S. Low, "A global maximum power point tracking scheme employing DIRECT search algorithm for photovoltaic systems," *IEEE Trans. Ind. Electron.*, vol. 57, no. 10, pp. 3456–3467, Oct. 2010.
- [6] Bader N. Alajmi, Khaled H. Ahmed, Stephen J. Finney, and Barry W. Williams, "A Maximum Power Point Tracking Technique for Partially Shaded Photovoltaic Systems in Microgrids," IEEE Transactions On Industrial Electronics, April 2013.
- [7] Pandiarajan N., Ramaprabha R., Ranganath Muthu, —Application of circuit model for photovoltaic energy conversion systemsll, research article.
- [8] Joachim Holtz and Bernd Beyer. Optimal synchronous pulsewidth modulation with a trajectory tracking scheme for high dynamic performance. *IEEE APEC'92*, pages 147–154, 1992.
- [9] Milan Pradanovic & Timothy Green, —Control and filter design of three phase inverter for high power quality grid connection, — IEEE transactions on Power Electronics, Vol.18. pp.1- 8, January 2003.
- [10] Sun, J.: Small-signal modeling of variable-frequency pulse-width modulators. *IEEE Trans. Aerosp. Electron. Syst.* **38**(3), 1104–1108 (2002)
- [11] Metin Kesler and Engin Ozdemir. "Synchronous-Reference-Frame-Based Control Method Under Unbalanced and Distorted Load Conditions ," 2011 , IEEE Transactions on Industrial Electronics, Vol. 58.
- [12] Miss. Sangita R Nandurkar , Mrs. Mini Rajeev. "Design and Simulation of three phase Inverter for grid connected Photovoltaic systems ," 2012 Proceedings of Third Biennial National Conference, NCNTE.
- [13] Zhou Dejia, Zhao Zhengming, Mohamed Eltawil and Yuan Liqiang. "Design and Control of a Three-Phase Grid-Connected Photovoltaic System," 2008 IEEE .
- [14] V. Kaura and V. Blasko, "Operation of a phase locked loop system under distorted utility conditions," *IEEE Trans. Ind. Appl.*, vol. 33, no. 1, pp. 58– 63, Jan./Feb. 1997.
- [15] L. R. Limongi, R. Bojoi, C. Pica, F. Profumo, and A. Tenconi, "Analysis and comparison of phase locked loop techniques for grid utility applications," in *Proc. PCC APOS*, Nagoya, Japan, 2007, pp. 674–681.